NeuroImage: Clinical 28 (2020) 102409

Contents lists available at ScienceDirect

NeuroImage: Clinical

journal homepage: www.elsevier.com/locate/ynicl

Longitudinal functional connectivity changes related to dopaminergic decline in Parkinson's disease

Weihua Li[a,b,*], Nick P. Lao-Kaim[a], Andreas-Antonios Roussakis[a], Antonio Martín-Bastida[a,c], Natalie Valle-Guzman[d], Gesine Paul[e,f], Eyal Soreq[g], Richard E. Daws[g], Tom Foltynie[h], Roger A. Barker[d], Adam Hampshire[g], Paola Piccini[a]

[a] Centre for Neurodegeneration and Neuroinflammation, Division of Brain Sciences, Imperial College London, London W12 0NN, United Kingdom
[b] Department of Radiology, Xuanwu Hospital, Capital Medical University, Beijing 100053, China
[c] Department of Neurology and Neurosciences, Clínica universidad de Navarra, Pamplona-Madrid, Spain
[d] John Van Geest Centre for Brain Repair, University of Cambridge, Cambridge CB2 0PY, United Kingdom
[e] Translational Neurology Group, Department of Clinical Sciences, Wallenberg Neuroscience Centre, Lund University, Lund 221 84, Sweden
[f] Division of Neurology, Department of Clinical Sciences, Lund University, Skåne University Hospital, Lund 22185, Sweden
[g] Imperial College London, Division of Brain Sciences, Computational Cognitive & Clinical Neuroimaging Lab (C^3NL), London W12 0NN, United Kingdom
[h] Sobell Department of Motor Neuroscience, UCL Institute of Neurology, National Hospital for Neurology and Neurosurgery, London WC1N 3BG, United Kingdom

ARTICLE INFO

Keywords:
Parkinson's disease
Resting-state functional magnetic resonance imaging
Functional connectivity
^{11}C-PE2I
Dopamine transporter

ABSTRACT

Background: Resting-state functional magnetic resonance imaging (fMRI) studies have demonstrated that basal ganglia functional connectivity is altered in Parkinson's disease (PD) as compared to healthy controls. However, such functional connectivity alterations have not been related to the dopaminergic deficits that occurs in PD over time.

Objectives: To examine whether functional connectivity impairments are correlated with dopaminergic deficits across basal ganglia subdivisions in patients with PD both cross-sectionally and longitudinally.

Methods: We assessed resting-state functional connectivity of basal ganglia subdivisions and dopamine transporter density using ^{11}C-PE2I PET in thirty-four PD patients at baseline. Of these, twenty PD patients were rescanned after 19.9 ± 3.8 months. A seed-based approach was used to analyze resting-state fMRI data. ^{11}C-PE2I binding potential (BP_{ND}) was calculated for each participant. PD patients were assessed for disease severity.

Results: At baseline, PD patients with greater dopaminergic deficits, as measured with ^{11}C-PE2I PET, showed larger decreases in posterior putamen functional connectivity with the midbrain and pallidum. Reduced functional connectivity of the posterior putamen with the thalamus, midbrain, supplementary motor area and sensorimotor cortex over time were significantly associated with changes in DAT density over the same period. Furthermore, increased motor disability was associated with lower intraregional functional connectivity of the posterior putamen.

Conclusions: Our findings suggest that basal ganglia functional connectivity is related to integrity of dopaminergic system in patients with PD. Application of resting-state fMRI in a large cohort and longitudinal scanning may be a powerful tool for assessing underlying PD pathology and its progression.

1. Introduction

Parkinson's disease (PD) is characterised by progressive loss of dopaminergic neurons in the substantia nigra and subsequent dysfunction of dopamine neurotransmission in the striatum (Nurmi et al., 2001; Eshuis et al., 2006). The presynaptic dopamine transporter (DAT) is a plasma membrane transporter that is localised exclusively in dopamine neurones (Piccini, 2003). Hence, DAT availability measured with DAT-specific radioligands and Positron Emission Tomography (PET) is one measure of nigrostriatal dopaminergic integrity (Shih et al., 2006; Pavese and Brooks, 2009). Previous longitudinal studies have demonstrated an annualized rate of reduction in striatal DAT binding of approximately 6–13% in patients with PD compared with 0–2.5% in healthy controls (Nurmi et al., 2000; Marek et al., 2001; Parkinson Study, 2002). The reduction in striatal DAT binding correlates with increasing disability in patients with PD (Seibyl et al., 1995; Li et al.,

* Corresponding author.
E-mail address: paola.piccini@imperial.ac.uk (W. Li).

https://doi.org/10.1016/j.nicl.2020.102409
Received 16 April 2020; Received in revised form 24 August 2020; Accepted 30 August 2020
Available online 02 September 2020

2017).

Resting-state functional magnetic resonance imaging (fMRI) offers a means of assessing the status of functional networks within the brain without the confounding influence of task performance (Fox and Greicius, 2010). It has been demonstrated that functional changes within the basal ganglia network can differentiate patients with PD from healthy controls (Szewczyk-Krolikowski et al., 2014), and are responsible for the cardinal motor features of PD (Wu et al., 2012). Hacker et al. (2012) reported lower striatal functional connectivity with the thalamus, midbrain, pons and cerebellum in patients with PD. Another study using a more spatially refined analysis found reduced functional connectivity between the posterior putamen and the sensorimotor cortex while functional connectivity was increased between the anterior putamen and the inferior parietal cortex (Helmich et al., 2010). It has been shown that functional connectivity in PD improves across striatal subdivisions under regular dopaminergic replacement therapy (Bell et al., 2015), suggesting that striatal functional connectivity is dependent on the integrity of dopaminergic system (Surmeier et al., 2010). For the substantia nigra, it was found that functional connectivity is decreased to the putamen in PD patients compared to healthy controls (Ellmore et al., 2013).

There are few studies assessing longitudinal changes in resting-state functional connectivity in PD patients (Olde Dubbelink et al., 2014; Manza et al., 2016). Olde Dubbelink et al. (2014) reported a gradual loss of global resting-state functional connectivity in PD, mainly in sensorimotor cortex, over the course of three years, which was modestly related to motor deficits (Olde Dubbelink et al., 2014). However, it is unclear how changes in resting-state functional connectivity are related to dopaminergic decline in patients with PD over time.

The primary aim of this study was to examine whether functional connectivity impairments are correlated with dopaminergic deficits across basal ganglia subdivisions in patients with PD both cross-sectionally and longitudinally. Here, we used resting-state fMRI to assess functional connectivity in thirty-four PD patients and fifteen age-matched healthy controls. To estimate DAT binding we used ^{11}C-PE2I PET, a highly specific radioligand which has been shown to be closely associated with PD motor severity and progression (Li et al., 2017). We hypothesized that longitudinal changes in resting-state functional connectivity of basal ganglia subdivisions would be associated with reductions in DAT binding and increasing motor disability in PD patients.

2. Method

2.1. Participants

Patients with PD were recruited from the Transeuro programme cohort (FP7 EC http://www.transeuro.org.uk/). All had a diagnosis of idiopathic PD in accordance with Queen Square Brain Bank criteria (Lees et al., 2009). A total of thirty-four patients with PD (PD_{BL}) completed ^{11}C-PE2I PET, structural MRI and resting-state fMRI scans at baseline, however four were excluded from the current analyses due to significant head motion. Of these, twenty PD patients completed follow-up measures after an interval of 19.9 ± 3.8 months, hereby referred to as the PD follow-up subgroup (PD_{FU}). From this group, three patients were excluded due to severe signal loss, and two patients were excluded due to excessive head motion during resting-state fMRI. Therefore, a total of fifteen patients were included in the longitudinal analysis.

Motor severity was assessed by two experienced clinicians using the motor sub-score of the Unified Parkinson's Disease Rating Scale (UPDRS-part III) (Goetz et al., 2008) and the Hoehn and Yahr staging scale (Hoehn and Yahr, 1967) whilst they were in an "off" medication state. We further subdivided the UPDRS-part III into tremor and bradykinesia-rigidity sub-scores. A total of fifteen age- and gender-matched healthy controls completed structural MRI and resting-state fMRI scans at baseline. None of the participants scored < 26 on the Mini-Mental State Examination (MMSE), had atypical or secondary Parkinsonism, or were ineligible for MRI and PET scanning (claustrophobia, metallic implants, pregnancy or breastfeeding, recent exposure to ionising radiation). All participants gave written informed consent in accordance with the Declaration of Helsinki. All aspects of the study were approval from the appropriate research ethics committees of the UK (REC 12/EE/0096 & 10/H0805/73) and Sweden (EPN 2013/758 & IK 2013/685) National Research Ethics Service Committee.

2.2. Image acquisition

All scans were conducted at the Invicro Imaging Centre (Hammersmith Hospital Campus, London). During scans, participants were positioned supine; head movement was minimised using memory foam padding and video monitoring utilised to aid detection and subsequent repositioning.

MRI scans were performed on a 3T Siemens Magnetom Trio with 32-channel phased-array head coil. High resolution structural images were acquired using a 3-dimensional T1-weighted sagittal magnetization-prepared rapid gradient-echo sequence (MPRAGE: TR/TE = 2300/2.98 ms; TI = 900 ms; FA = 9°; bandwidth = 240 Hz/Px; GRAPPA acceleration factor = 2; slice thickness = 1 mm (no gap); FoV = 240 × 256 mm; matrix size = 240 × 256) in which one whole brain volume was obtained consisting of 160 slices lasting 301 s. Resting-state fMRI scans were acquired for 368 s using a T2*-weighted single-shot gradient-echo echo planar imaging (EPI) sequence (TR/TE = 2500/31.3 ms; FA = 80°; bandwidth = 2298 Hz/Px; GRAPPA acceleration factor = 2; slice thickness = 3 mm (no gap); FoV = 192 × 192 mm; matrix size = 64 × 64). 144 brain volumes were obtained per individual, each consisting of 45 interleaved axial slices acquired parallel to the AC-PC line. Participants were instructed to remain as still as possible with their eyes closed, and to avoid falling asleep during the scan.

^{11}C-PE2I (N-(3-iodopro-2E-enyl)-2β-carbomethoxy-3β-(4′-methylphenyl)nortropane) PET imaging was conducted on a Siemens Biograph TruePoint HI-REZ 6 PET/CT system. Radioligand volumes (^{11}C-PE2I = 350 MBq) were prepared to 10 ml using saline solution and administered intravenously as single bolus injections followed immediately by 10 ml saline flush. Administration was at 1 ml/sec. Dynamic emission data were acquired continuously for 90 min post-injection then reconstructed into 26 temporal frames using a filtered back-projection algorithm (direct inversion Fourier transform; matrix size = 128x128, zoom = 2.6, 5 mm transaxial Gaussian filter, pixel size = 2 mm isotropic). A low-dose CT transmission scan (0.36 mSv) was acquired for attenuation correction prior to the injection of ^{11}C-PE2I. PD patients were instructed to withdraw their dopaminergic medication at least 24 h prior to scanning for standard release preparations and 48 h for prolonged release medications (Li et al., 2017).

2.3. Image preprocessing

Standard image preprocessing of resting-state fMRI was performed using Statistical Parametric Mapping (SPM12, Wellcome Trust Centre for Neuroimaging, London, UK, http://www.fil.ion.ucl.ac.uk/spm/). Each participant's structural image was segmented for cerebrospinal fluid (CSF) and white matter (WM). Resting-state fMRI data were slice-time corrected, realigned to the first image using rigid-body motion transforms and co-registered to the structural image. For every time point t, the framewise displacement (FD) was calculated, and every time point that exceeded a pre-defined head motion limit (FD (t) > 0.5 mm) was removed (Power et al., 2012). The FD values were later used as nuisance regressors and confounding covariates in the individual and group-level analyses, respectively. Then, a 'scrubbing' procedure was performed using the '*fsl_motion_outliers*' tool in FSL to remove the time points affected by head motion (motion spike) (Power et al., 2012). A nuisance regression was conducted using a Volterra

series expansion (i.e. Friston 24-parameter model) of the motion estimates (six motor parameters, six motion parameters one time point before, and the 12 corresponding squared items) (Friston et al., 1996), the time series of CSF and WM, the motion spike and FD values as regressors. The structural image was then spatially normalized to a Montreal Neurological Institute (MNI) space (Mazziotta et al., 1995) using affine registration followed by non-linear transformation. The estimated warps were then applied to the corresponding noise-corrected functional images for each participant and smoothed with a 6-mm full-width-at-half-maximum (FWHM) Gaussian filter. A temporal band-pass filtering of 0.009 Hz $< f <$ 0.08 Hz was applied to the time series data to reduce the effects of low-frequency drift and high-frequency noise (Lowe et al., 1998; Fair et al., 2007).

PET and corresponding structural images were preprocessed and analyzed using MIAKAT^{TM} v3.4.2. (Molecular Imaging and Kinetic Analysis Toolbox, Imanova Ltd., London) (Gunn et al., 2016), which implements FSL (FMRIB Image Analysis Group, Oxford, UK) (Jenkinson et al., 2012), SPM and in-house preprocessing and kinetic modelling procedures. Structural images were brain extracted, segmented and rigid body registered to the MNI template. Dynamic PET images were corrected for intra scan head movement using frame-to-frame rigid registration with a pre-specified reference frame (frame = 16). Realigned frames between 10 and 90 min were summed to obtain signal averaged (ADD) images, which were co-registered to the corresponding structural image. These co-registration matrices were then applied to the realigned dynamic PET frames and region-of-interest (ROI) maps overlaid to generate regional time-activity curves (TACs). Regional non-displaceable binding potential (BP_{ND}) was calculated using the simplified reference tissue model (SRTM) (Lammertsma and Hume, 1996). Cerebellar grey matter was used as a reference region under the assumption that it has negligible DAT density (Hall et al., 1999; Halldin et al., 2003).

Striatal ROIs were manually segmented for each participant on structural MR images displayed in standard space using ROI tools in Analyze11.0 (Biomedical Imaging Resource, Mayo Clinic). Striatal ROIs were defined bilaterally in the (i) caudate; (ii) anterior putamen; and (iii) posterior putamen on the axial plane followed by trace checks on the coronal plane. The putamen was subdivided into anterior and posterior parts using a marker placed on the coronal plane at the level of the anterior commissure (Tziortzi et al., 2011). Substantia nigra and cerebellar ROIs were obtained from the CIC atlas (CIC Atlas v2.0; GlaxoSmithKline, Clinical Imaging Centre, London, UK) (Fig. 1). Rigid-body registration parameters were applied to the grey and white matter segmentation images to enable automatic masking of cerebellar grey matter.

2.4. Functional connectivity analysis

Resting-state functional connectivity was assessed using a seed-based approach with bilateral caudate, anterior putamen, posterior putamen and substantia nigra as seeds. Functional connectivity maps were obtained by computing the Pearson's correlation coefficient between the averaged time series of each seed region and that of all other voxels in the brain for each individual participant. These correlation coefficients were converted to normally distributed values using Fisher's *r*-to-Z transform for use at the group level. The individual z-maps were entered into a random effect one-sample *t-test* to identify brain regions showing significant positive correlations with the seed ROIs. Then, the individual z-maps were entered into a random effect two-sample *t-test* to identify differences in functional connectivity between groups (PD_{BL} *vs.* healthy controls at baseline; PD_{BL} *vs.* PD_{FU}). Statistical maps were thresholded at voxel-level $p_{FWE} < 0.05$ and cluster-level $p_{FDR} < 0.05$.

2.5. Multiple regression analysis

For patients with PD at baseline (n = 30), to investigate the associations between regional ^{11}C-PE2I BP_{ND} and functional connectivity of the seed regions, voxel-based multiple regression analysis was conducted using functional connectivity maps as the dependent variable, the regional ^{11}C-PE2I BP_{ND} as the independent variable, and age/gender as nuisance covariates. The FD, averaged across the entire time series, was also entered as a covariate to minimize the potential effect of motion-related variance on group inference. The correlation analysis was assessed using *t*-statistics. To explore correlates of functional connectivity with disease severity, multiple regression analysis was performed with UPDRS-III, bradykinesia-rigidity and tremor sub-scores entered as covariates of interest. All statistical maps were thresholded at voxel-level $p < 0.001$ uncorrected and cluster-level false discovery rate corrected $p_{FDR} < 0.05$.

We also assessed how changes in functional connectivity over time correlated with changes in ^{11}C-PE2I BP_{ND} over time. Difference functional connectivity maps were created by voxel-based subtraction (Δ: follow-up – baseline) and entered into a multiple regression analysis as the dependent variable with Δ^{11}C-PE2I BP_{ND} as the independent variable (Supplementary Material Table 1 provides information on percentage annual decrease in regional ^{11}C-PE2I BP_{ND} for the PD_{FU} subgroup), and age at baseline and gender as nuisance covariates. In addition, to examine how changes in functional connectivity correlated with changes in motor disability over time, multiple regression analysis was also performed with ΔUPDRS-III, Δbradykinesia-rigidity and Δtremor sub-scores entered as covariates of interest. All statistical maps

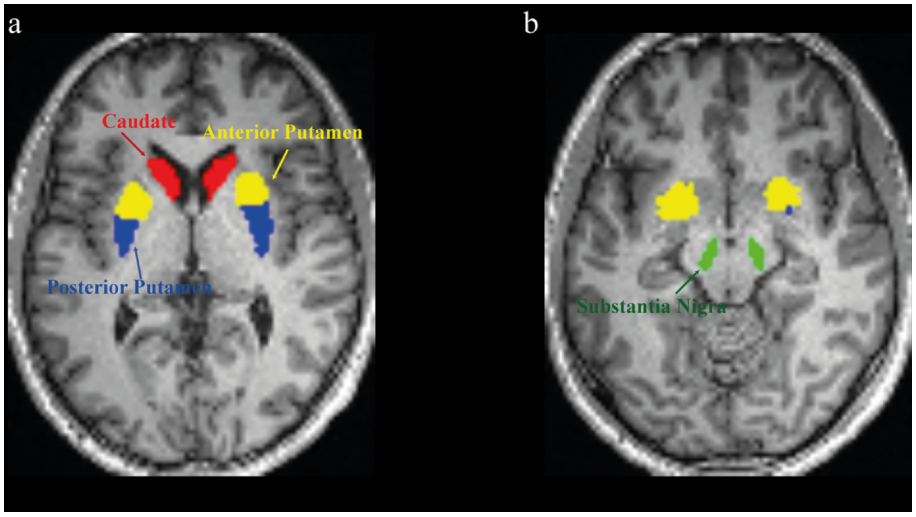

Fig. 1. Seeds region-of-interest defined in a representative PD patient. Region-of-interests were manually segmented for each participant's on structural image displayed in standard space. Brain left is shown on the image left. Four seeds region-of-interest were defined in each subject: caudate (a, in red), anterior putamen (a, in yellow), posterior putamen (a, in blue) and substantia nigra (b, in green). (For interpretation of the references to colour in this figure legend, the reader is referred to the web version of this article.)

Table 1
Demographic and clinical information for all study participants at baseline (*PD: n = 30; HC: n = 15*) and for the PD subgroup at baseline and 19.9 ± 3.8 months follow-up (PD_{FU}: *n = 15*). Independent-samples *t-test* was used to assess the difference between PD and healthy controls at baseline. For the PD follow-up group, Wilcoxon signed-rank and paired-samples *t-test* were used to assess the difference between baseline and follow-up.

Baseline: PD (n = 30); HC (n = 15)	PD	HC	Statistic	*p*
Gender (M:F)	24:6	8 : 7		
Age (years) [a]	55.4 ± 7.1	53.15 ± 11.4	$t(19.674) = 0.696$	0.494
Disease duration (years) [a]	5.8 ± 2.2	N/A		
UPDRS-III [a]	31.3 ± 10.6	N/A		
UPDRS-III Bradykinesia-Rigidity [a]	22.4 ± 8.1	N/A		
UPDRS-III Tremor [a]	6.2 ± 5.3	N/A		
Hoehn & Yahr Scale [b]	2.0 (0.0)	N/A		
LED [a]	670.3 ± 361.8	N/A		
Follow-Up: PD_{FU} (n = 15)	Baseline	Follow-Up	Statistic	*p*
Gender (M:F)	12:3	12:3		
Age (years) [a]	53.0 ± 7.2	54.7 ± 7.1	$t(14) = 26.445$	< 0.001 *
Disease duration (years) [a]	6.0 ± 2.2	7.7 ± 2.0	$t(14) = 26.234$	< 0.001 *
UPDRS-III [a]	31.4 ± 12.0	35.9 ± 10.9	$t(14) = 2.003$	0.065
UPDRS-III Bradykinesia-Rigidity [a]	22.4 ± 9.6	25.2 ± 8.9	$t(14) = 1.925$	0.075
UPDRS-III Tremor [a]	6.9 ± 4.5	8.3 ± 4.2	$t(14) = 1.514$	0.152
Hoehn & Yahr Scale [b]	2.0 (0.0)	2.0 (0.0)	$Z = 1.7$	0.083
LED [a]	771.7 ± 386.5	906.3 ± 235.7	$t(14) = 2.156$	0.046 *

[a] Data are presented as Mean ± SD.
[b] Data are presented as Median (Interquartile Range).
* Indicates $p < 0.05$
LED = L-dopa equivalent dose (mg).
UPDRS = Unified Parkinson's disease rating scale.
The UPDRS and H&Y scale were assessed in the practically defined off-medication state.

were thresholded at voxel-level $p < 0.001$ uncorrected and cluster-level false discovery rate corrected $p_{FDR} < 0.05$.

3. Results

Demographics and clinical characteristics of the study participants are summarised in Table 1.

3.1. Resting-state functional connectivity in patients with PD and healthy controls

Resting-state functional connectivity of basal ganglia subdivisions at baseline in patients with PD was generally consistent with previous studies (Fig. 2). The caudate was connected to the anterior/posterior cingulate cortex and thalamus. The anterior putamen and posterior putamen exhibited similar patterns of functional connectivity with the supplementary motor area (SMA), sensorimotor cortex, thalamus and a contiguous region of grey matter extending from the thalamus through the midbrain, pons and cerebellum. The substantia nigra showed functional connectivity with the caudate, putamen, globus pallidus, thalamus and cerebellum. The functional connectivity patterns of the healthy controls were roughly similar to that of the PD patients (Supplementary Material Fig. 1). To ensure that group-level results were not influenced by spurious correlations as a result of in-scanner head movement, we compared the mean FD between the groups (healthy controls *vs.* PD at baseline, $p = 0.577$; PD at baseline *vs.* PD at follow up, $p = 0.493$), suggesting that head movement did not differentially alter resting-state functional connectivity across groups (Supplementary Material Table 2).

At baseline, voxel-based comparisons of functional connectivity maps for each of the four seed regions between PD patients and healthy controls were conducted. Both the caudate and the anterior putamen showed decreased intraregional functional connectivity for the PD group as compared to HC (Fig. 3a and 3b), while the posterior putamen showed the opposite pattern. In the PD group, the posterior putamen exhibited an enhanced intraregional functional connectivity intermediate between anterior and posterior putamen (Fig. 3c). PD patients exhibited reduced functional connectivity between the substantia nigra and the thalamus and pallidum as well as with smaller clusters located within the caudate and putamen (Fig. 3d).

Functional connectivity maps of each of the four seed regions were also compared between baseline and follow-up for the PD patients. We found a time-related decrease of functional connectivity between the anterior putamen and sensorimotor cortex (Fig. 4a). In addition, the posterior putamen showed decreased functional connectivity with the anterior putamen and the posterior putamen (intraregional), as well as smaller clusters in the caudate, thalamus and midbrain (Fig. 4b). There were no significant differences in caudate and substantia nigra functional connectivity between the two time points.

3.2. Correlation between basal ganglia functional connectivity and ^{11}C-PE2I BP_{ND} and clinical measures: multiple regression analyses

At baseline, voxel-based multiple regression analysis of posterior putamen functional connectivity maps revealed clusters in the midbrain and pallidum showing a significant positive correlation with posterior putamenal ^{11}C-PE2I BP_{ND} (Fig. 5a, Table 2). No significant correlations between functional connectivity maps of other seed regions (caudate, anterior putamen and substantia nigra) and ^{11}C-PE2I BP_{ND} values were observed. Furthermore, we did not find any significant correlations between the functional connectivity of basal ganglia subdivisions and clinical scores.

Longitudinally, voxel-based analysis of the change in posterior putamen functional connectivity (Δ: follow-up – baseline) revealed clusters showing significant positive correlations with Δ^{11}C-PE2I BP_{ND} in the posterior putamen. These clusters were found in the left thalamus and a contiguous region of grey matter extending from the thalamus, through the midbrain, as well as in the SMA, precentral gyrus and postcentral gyrus (Fig. 5b, Table 2). Furthermore, clusters showing significant positive correlations between Δposterior putamen functional connectivity and Δbradykinesia-rigidity sub-scores were found in the right posterior putamen (Fig. 5c, Table 2). No other significant results

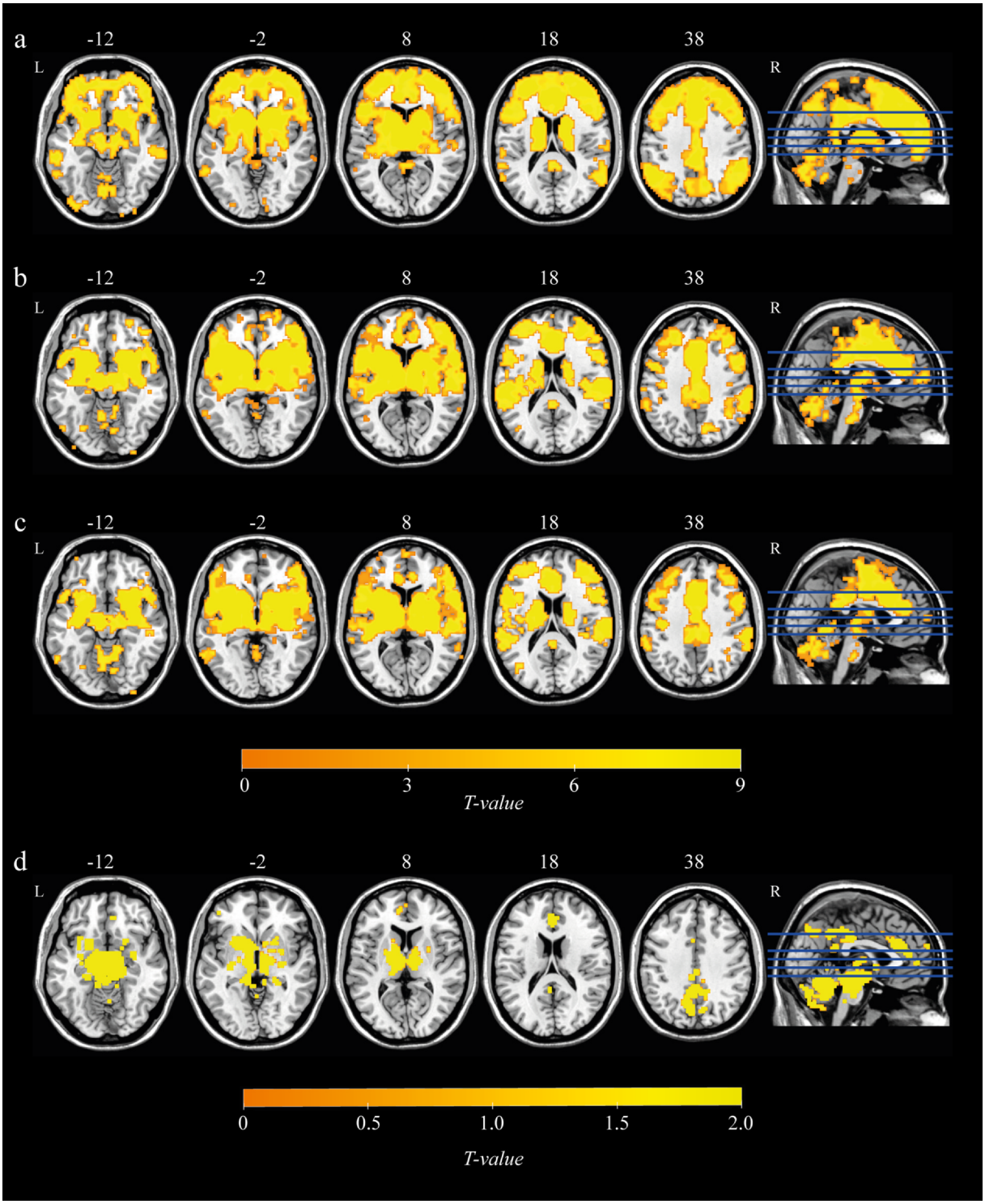

Fig. 2. Resting-state functional connectivity of basal ganglia subdivisions (a) caudate, (b) anterior putamen, (c) posterior putamen and (d) substantia nigra in patients with PD. All statistical maps ($p_{FWE} < 0.05$ *FWE*-corrected at voxel-level, and $p_{FDR} < 0.05$ *FDR*-corrected at cluster-level) are overlaid on a T1-weighted MNI template. L, left; R, right.

were found for longitudinal analyses.

4. Discussion

Our findings demonstrate that resting-state functional connectivity of the posterior putamen is associated with the integrity of the dopaminergic system in patients with PD. PD patients with more severe dopaminergic deficits showed larger decreases in posterior putamen functional connectivity with the midbrain and pallidum. In addition, longitudinal comparison between the two timepoints revealed that patients with PD showed reduced functional connectivity of the posterior putamen with the thalamus and midbrain. These functional connectivity changes were correlated with dopamine deficits of disease progression. Lastly, increased motor disability was associated with lower intraregional functional connectivity of the posterior putamen. These results suggest an essential role of dopamine in striatal function

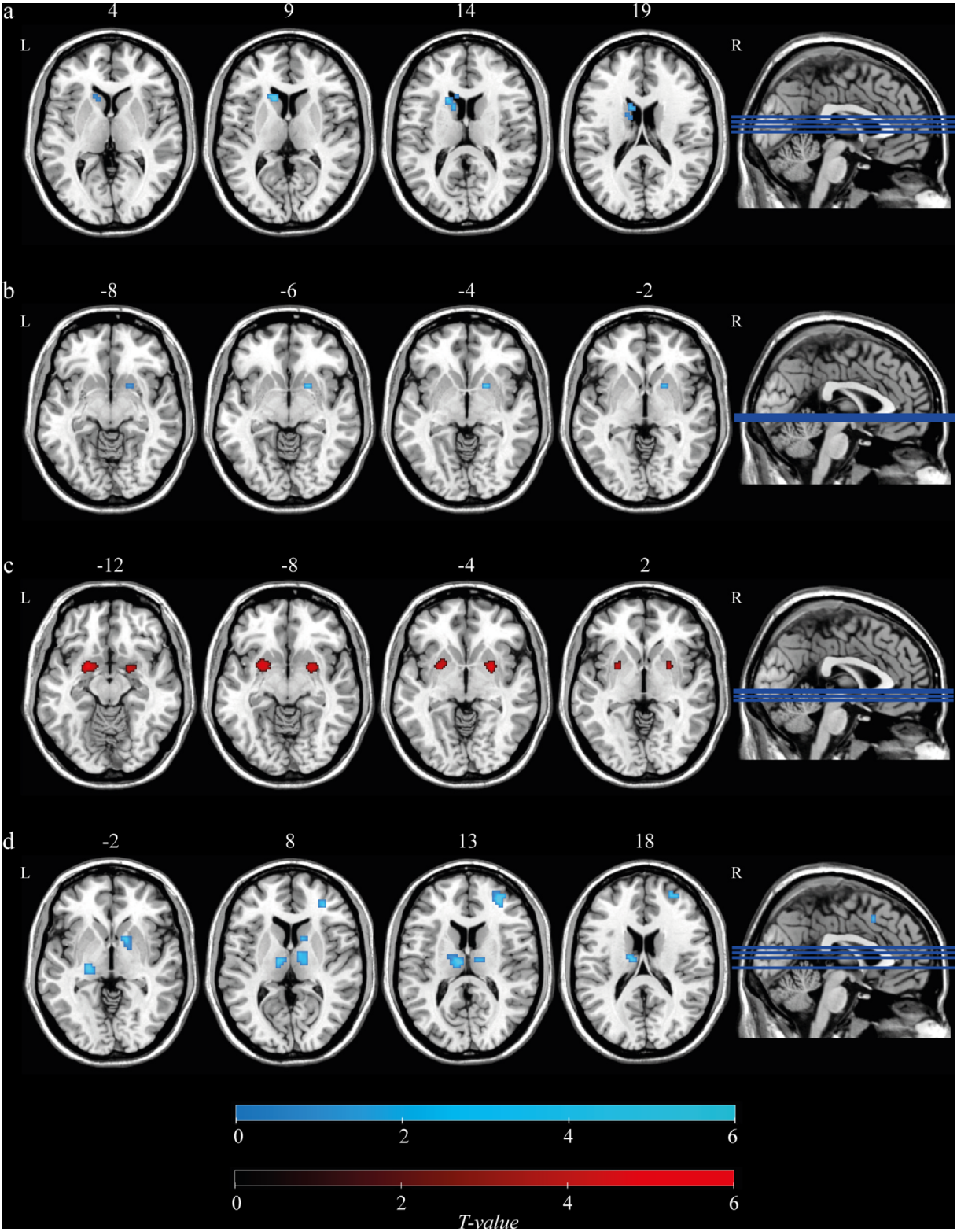

Fig. 3. Group differences in resting-state functional connectivity between PD patients and healthy controls (HC) (a) caudate, (b) anterior putamen, (c) posterior putamen and (d) substantia nigra. Blue and red colours represent HC > PD and PD > HC, respectively. All statistical maps ($p_{FWE} < 0.05$ *FWE*-corrected at voxel-level, and $p_{FDR} < 0.05$ *FDR*-corrected at cluster-level) are overlaid on a T1-weighted MNI template. L, left; R, right. (For interpretation of the references to colour in this figure legend, the reader is referred to the web version of this article.)

and demonstrate that resting-state functional connectivity of basal ganglia subdivisions is compromised by the dopaminergic pathology of PD.

A previous study using resting-state fMRI demonstrated reduced functional connectivity within the basal ganglia of patients with early PD as compared to patients with Alzheimer's disease (AD) and healthy controls (Rolinski et al., 2015). These changes were not seen in AD patients, suggesting that aberrant functional connectivity within the

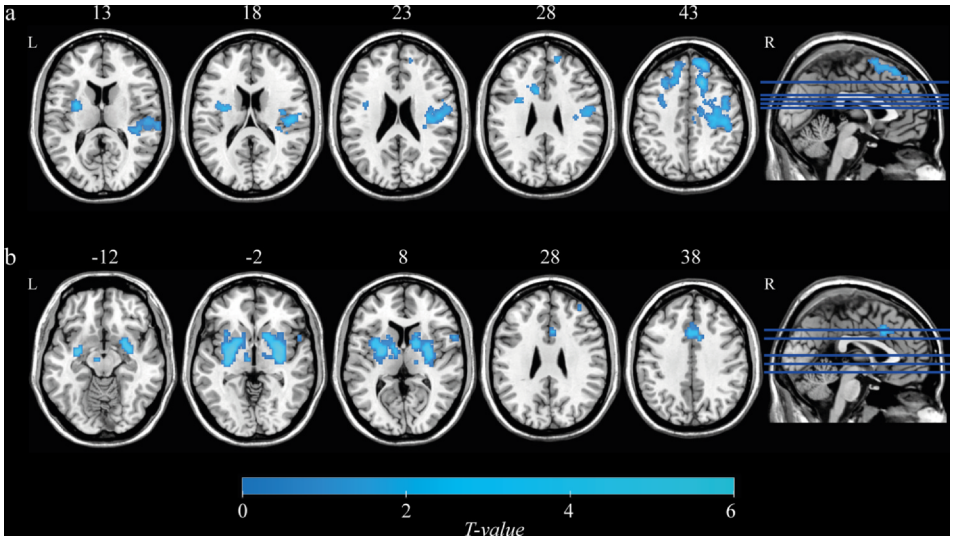

Fig. 4. Changes in resting-state functional connectivity in patients with PD between two timepoints (a) anterior putamen and (b) posterior putamen. Blue colour represents the decreased functional connectivity of PD patients at follow-up compared to baseline. All statistical maps ($p_{FWE} < 0.05$ *FWE*-corrected at voxel-level, and $p_{FDR} < 0.05$ *FDR*-corrected at cluster-level) are overlaid on a T1-weighted MNI template. L, left; R, right. (For interpretation of the references to colour in this figure legend, the reader is referred to the web version of this article.)

basal ganglia of PD patients is disease specific. In the current study, reduced intraregional functional connectivity of the caudate and the anterior putamen was found in PD patients compared to healthy controls. In contrast, we found increased intraregional functional connectivity of the posterior putamen, suggesting a compensatory mechanism that develops in response to marked dopamine decline in the posterior putamen (Helmich et al., 2010). It has been demonstrated that noradrenaline, serotonin and acetylcholine are also affected in PD, although to a lesser degree than dopamine, thus it is possible that other neurotransmitter systems might play a role in mediating changes in basal ganglia functional connectivity patterns (Shine et al., 2019). Lastly, we found reduced substantia nigra functional connectivity with the thalamus extending to the caudate and putamen, which is generally consistent with results reported by Wu et al. (2012) who also showed additional reductions to the globus pallidus, insula and SMA in PD patients as compared to the healthy controls (Wu et al., 2012).

Previous studies have demonstrated significant correlations between motor symptomatology and altered functional connectivity of basal ganglia subdivisions in patients with PD (Wu et al., 2009; Hacker et al., 2012; Agosta et al., 2014). Greater severity of UPDRS-III motor scores appears to be associated with reduced functional connectivity between the striatum and midbrain (Hacker et al., 2012) and increased functional connectivity between the putamen and occipital/parietal cortex (Agosta et al., 2014), suggesting a potential role basal ganglia functional connectivity alterations in the occurrence of motor impairment (Cerasa et al., 2016). However, in the current study, baseline functional connectivity did not correlate with any clinical measures of motor severity. In line with our findings, a study examined functional connectivity within the basal ganglia network also did not find any significant correlations between the basal ganglia network connectivity and clinical measures (Szewczyk-Krolikowski et al., 2014). They suggested that functional connectivity alterations of basal ganglia network may be a trait biomarker of PD, reflecting a constitutional fault of the network and not the resulting motor symptoms (Szewczyk-Krolikowski et al., 2014).

Postmortem and neuroimaging studies have demonstrated that the posterior putamen suffers most from degeneration of the nigrostriatal dopaminergic pathway (Kish et al., 1988; Nurmi et al., 2001; Bruck et al., 2006; Helmich et al., 2010). The most consistent finding across resting-state fMRI studies in patients with PD appears to be a reduction of posterior putamenal functional connectivity that correlates with greater motor impairment (Herz et al., 2014). Few studies have examined how striatal functional connectivity varies with dopaminergic deficit in PD. One study found that reduced functional connectivity between the putamen and the midbrain was related to dopaminergic status in the striatum (Rieckmann et al., 2015) while another demonstrated that functional connectivity was modulated by striatal dopamine levels (Baik et al., 2014). Here, in thirty PD patients, we found that reduced functional connectivity between the posterior putamen and the midbrain was significantly associated with dopamine levels in the posterior putamen. In a preliminary analysis, we also found in a subset of fifteen PD patients that changes in this functional connectivity pattern correlated with changes in dopamine levels in the posterior putamen. Taken together, these findings suggest that resting-state functional connectivity of the posterior putamen may reflect impairment of the nigrostriatal dopaminergic projection in the PD brain.

Although PD is the most common form of parkinsonism, there are other atypical neurodegenerative conditions that mimic the clinical features of PD, such as multiple system atrophy (MSA) and progressive supranuclear palsy (PSP) (Politis, 2014). DAT radioligands with PET have shown promising sensitivity and specificity for distinguishing patients with parkinsonian syndromes from healthy controls (Antonini et al., 2001; Jakobson Mo et al., 2018). However, dopamine-specific radioligands cannot accurately differentiate between PD, MSA and PSP. Advanced MRI techniques, such as resting-state fMRI and arterial spin labeling (ASL), may therefore help to provide complementary information for more accurate differential diagnosis. Recently developed hybrid PET/MR systems allow simultaneous acquisition of MRI and PET data, which in theory enables more precise spatial co-registration and importantly offers greater convenience for motor impaired patients (Tondo et al., 2019). Indeed, combined acquisition of ASL and ^{18}F-FDG PET on a hybrid PET/MR system was recently shown to increase sensitivity in differentiating PD and MSA, based on changes in the caudate nucleus, pons and cerebellum (Ruan et al., 2019). Another study demonstrated a close relationship between global grey matter changes and the degeneration of striatal dopaminergic circuits in patients with PD (Choi et al., 2016). Taken together, as a non-invasive and more comprehensive approach, the combined use of advanced MRI and PET on hybrid scanners may play an increasingly important role for evaluating the underlying mechanisms of patients with PD.

This study has some limitations that need to be addressed. First, although our longitudinal results accord with well-founded predictions they were based on a relatively small number of PD participants and as such should be validated in larger samples. We believe that our findings provide promising new insights into changes in resting-state functional connectivity and their relation to DAT decline and motor dysfunction in PD patients. Second, only a single time interval of ~ 20 months was studied, thus future resting-state fMRI studies should be designed to evaluate patients more than twice and at longer intervals, which may provide additional evidence on the staging of PD progression and the

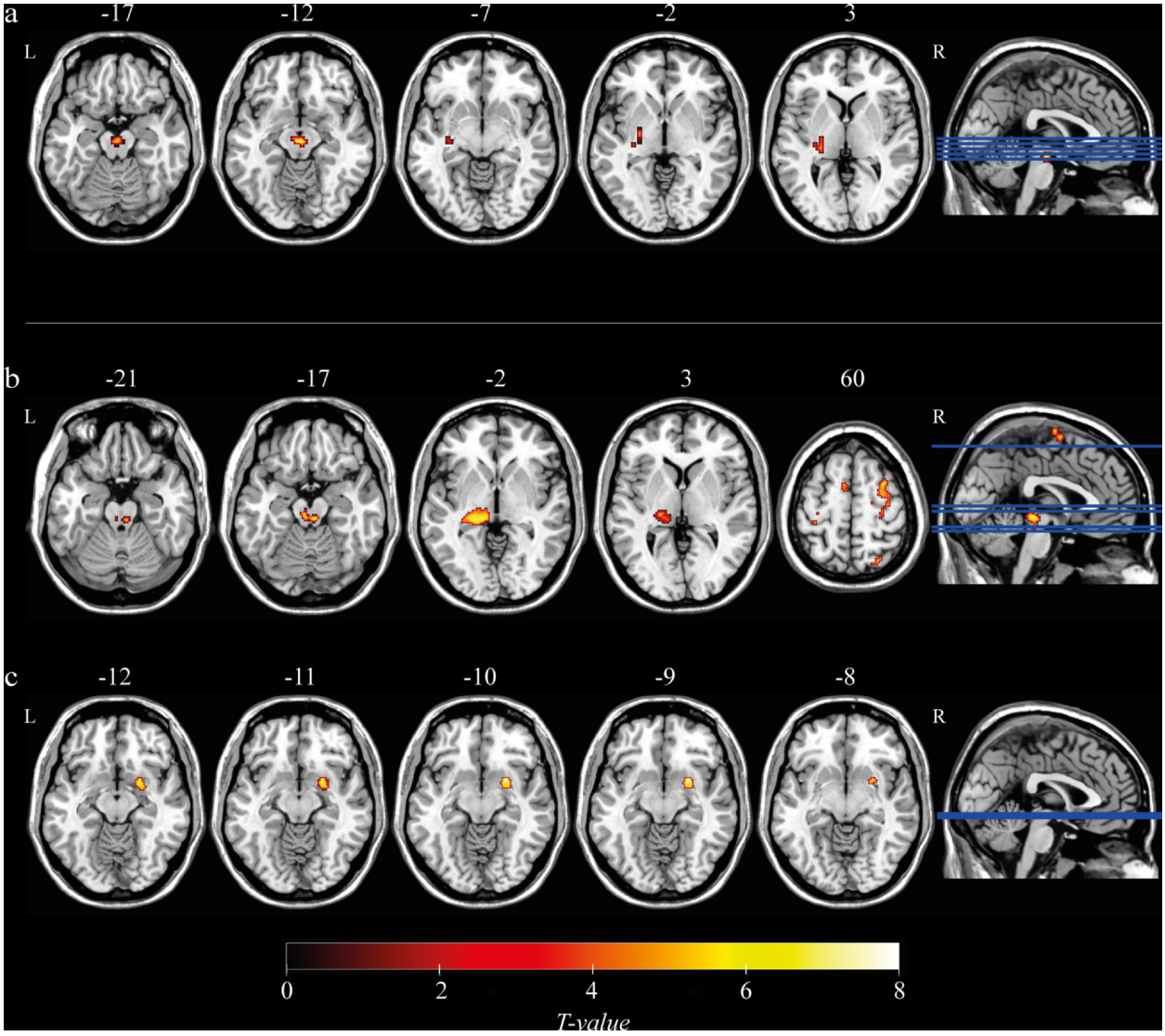

Fig. 5. Results of the voxel-based multiple regression analysis for PD patients at baseline (n = 30; a) and follow-up (n = 15; b and c). (a) The posterior putamen functional connectivity revealed clusters in the midbrain and pallidum, that showed a significant positive correlation with ^{11}C-PE2I BP_{ND} in the posterior putamen. (b) Changes in posterior putamen ^{11}C-PE2I-BP_{ND} are positively correlated with changes in functional connectivity between the posterior putamen and thalamus, midbrain, SMA, precentral gyrus and postcentral gyrus. (c) Changes in bradykinesia-rigidity sub-score are positively correlated with changes in posterior putamen intraregional functional connectivity. All statistical maps ($p < 0.001$ uncorrected at voxel-level, and $p_{FDR} < 0.05$ FDR-corrected at cluster-level) are overlaid on a T1-weighted MNI template. L. left; R, right.

Table 2
Clusters showing positive correlations between posterior putamen functional connectivity and ^{11}C-PE2I BP_{ND} and disease severity (Bradykinesia-Rigidity sub-score), as revealed by voxel-wise multiple regression analysis for all PD patients. Longitudinal multiple regression using difference maps (Δ: follow-up – baseline) from the PD_{FU} group are also shown.

Seed		Covariate of Interest	Cluster		Peak *T*	MNI Coordinates			Brain Region
			p Value*	*k*		*x*	*y*	*z*	
Posterior putamen	Baseline Analysis(n = 30)	^{11}C-PE2I BP_{ND}	0.027	22	4.65	0	−18	−12	Midbrain
	Follow-up Analysis(n = 15)	Δ ^{11}C-PE2I BP_{ND}	0.007	580	5.37	−4	−26	−8	Midbrain, extending into thalamus
			0.001	845	4.66	10	−4	72	Supplementary motor area
			0.031	376	4.39	−36	−36	54	Postcentral gyrus, extending into precentral gyrus
		Δ Bradykinesia-Rigidity sub-score	0.032	48	6.37	24	6	−10	Posterior putamen

Threshold of $p < 0.001$ uncorrected at voxel-level and $p < 0.05$ corrected for false discovery rate at cluster-level.
Coordinates of peak voxels (*x, y, z*) are given in Montreal Neurologic Institute (MNI) space.
*Indicates correction for false discovery rate.

relevance to dopaminergic deficit. Third, the current study did not control for the potential impact of PD-related atrophy on dopaminergic deficits and resting state functional connectivity. Previous studies in PD have shown a close relationship between atrophy and the degeneration of striatal dopaminergic circuits (Choi et al., 2016), but have failed to find an association with disruptions of functional connectivity (Helmich et al., 2010; Luo et al., 2014). Lastly, patients with PD in this study underwent scanning while in the practically-defined "off" medicated state, but the long-term impact of chronic dopaminergic treatment on resting-state functional connectivity still remains unclear and as such warrants further investigation in future studies.

5. Conclusion

In conclusion, our study demonstrates that functional connectivity of basal ganglia subdivisions in PD is closely related to both the integrity of the dopaminergic system and motor severity. Our findings suggest that basal ganglia functional connectivity in the resting-state may be a powerful imaging biomarker for assessing underlying PD pathology and its progression, and may offer a meaningful way to investigate the mechanisms whereby dopamine deficiency leads to motor symptoms.

Funding

The TransEuro study received funding from an FP7 EU Consortium. The Medical Research Council (MRC) co-funded the PET scans along with the FP7 EU Consortium. An NIHR award of Biomedical Research Centre to the University of Cambridge/ Addenbrooke's Hospital and Imperial College London supported part of this study. Travel of Lund patients with staff has been funded by local grants in addition to TransEuro (Swedish Parkinson Academy, Regional Academic Learning Grants, and Multipark).

CRediT authorship contribution statement

Weihua Li: Conceptualization, Data curation, Formal analysis, Investigation, Methodology, Software, Validation, Visualization, Writing - original draft, Writing - review & editing. **Nick P. Lao-Kaim:** Conceptualization, Data curation, Software, Writing - review & editing. **Andreas-Antonios Roussakis:** Conceptualization, Data curation. **Antonio Martín-Bastida:** Conceptualization, Data curation. **Natalie Valle-Guzman:** Conceptualization, Data curation. **Gesine Paul:** Conceptualization, Data curation, Writing - review & editing. **Eyal Soreq:** Software. **Richard E. Daws:** Software. **Tom Foltynie:** Conceptualization, Data curation, Writing - review & editing. **Roger A. Barker:** Conceptualization, Data curation, Funding acquisition, Writing - review & editing. **Adam Hampshire:** Methodology, Supervision, Writing - review & editing. **Paola Piccini:** Conceptualization, Data curation, Project administration, Resources, Supervision, Funding acquisition, Writing - review & editing.

Declaration of Competing Interest

The authors declare that they have no known competing financial interests or personal relationships that could have appeared to influence the work reported in this paper.

Acknowledgements

This article presents independent research funded by the FP7 EU Consortium and the MRC that is supported by the NIHR CRF and BRC at Imperial College Healthcare NHS Trust. The views expressed are those of the authors and not necessarily those of the funder, the NHS, the NIHR or the Department of Health. We are very grateful to the patients who took part in this study.

Ethical approval

All procedures performed in studies involving human participants were in accordance with the ethical standards of the institutional and/or national research committee and with the 1964 Helsinki declaration and its later amendments or comparable ethical standards.

Informed consent

Informed consent was obtained from all individual participants included in the study.

Submission declaration and verification

This work has not been published previously, and it is not under consideration for publication elsewhere. Its publication is approved by all authors and that, if accepted, it will not be published elsewhere in the same form, in English or in any other language, including electronically without the written consent of the copyright-holder.

Appendix A. Supplementary data

Supplementary data to this article can be found online at https://doi.org/10.1016/j.nicl.2020.102409.

References

Agosta, F., Caso, F., Stankovic, I., Inuggi, A., Petrovic, I., Svetel, M., Kostic, V.S., Filippi, M., 2014. Cortico-striatal-thalamic network functional connectivity in hemiparkinsonism. Neurobiol. Aging 35, 2592–2602.

Antonini, A., Moresco, R.M., Gobbo, C., De Notaris, R., Panzacchi, A., Barone, P., Calzetti, S., Negrotti, A., Pezzoli, G., Fazio, F., 2001. The status of dopamine nerve terminals in Parkinson's disease and essential tremor: a PET study with the tracer [11-C]FE-CIT. Neurol. Sci. 22, 47–48.

Baik, K., Cha, J., Ham, J.H., Baek, G.M., Sunwoo, M.K., Hong, J.Y., Shin, N.Y., Kim, J.S., Lee, J.M., Lee, S.K., Sohn, Y.H., Lee, P.H., 2014. Dopaminergic modulation of resting-state functional connectivity in de novo patients with Parkinson's disease. Hum. Brain Mapp. 35, 5431–5441.

Bell, P.T., Gilat, M., O'Callaghan, C., Copland, D.A., Frank, M.J., Lewis, S.J., Shine, J.M., 2015. Dopaminergic basis for impairments in functional connectivity across subdivisions of the striatum in Parkinson's disease. Hum. Brain Mapp. 36, 1278–1291.

Bruck, A., Aalto, S., Nurmi, E., Vahlberg, T., Bergman, J., Rinne, J.O., 2006. Striatal subregional 6-[18F]fluoro-L-dopa uptake in early Parkinson's disease: a two-year follow-up study. Mov. Disord. 21, 958–963.

Cerasa, A., Novellino, F., Quattrone, A., 2016. Connectivity changes in Parkinson's disease. Curr. Neurol. Neurosci. Rep. 16, 91.

Choi, H., Cheon, G.J., Kim, H.J., Choi, S.H., Kim, Y.I., Kang, K.W., Chung, J.K., Kim, E.E., Lee, D.S., 2016. Gray matter correlates of dopaminergic degeneration in Parkinson's disease: a hybrid PET/MR study using (18) F-FP-CIT. Hum. Brain Mapp. 37, 1710–1721.

Ellmore, T.M., Castriotta, R.J., Hendley, K.L., Aalbers, B.M., Furr-Stimming, E., Hood, A.J., Suescun, J., Beurlot, M.R., Hendley, R.T., Schiess, M.C., 2013. Altered nigrostriatal and nigrocortical functional connectivity in rapid eye movement sleep behavior disorder. Sleep 36, 1885–1892.

Eshuis, S.A., Maguire, R.P., Leenders, K.L., Jonkman, S., Jager, P.L., 2006. Comparison of FP-CIT SPECT with F-DOPA PET in patients with de novo and advanced Parkinson's disease. Eur. J. Nucl. Med. Mol. Imaging 33, 200–209.

Fair, D.A., Schlaggar, B.L., Cohen, A.L., Miezin, F.M., Dosenbach, N.U., Wenger, K.K., Fox, M.D., Snyder, A.Z., Raichle, M.E., Petersen, S.E., 2007. A method for using blocked and event-related fMRI data to study "resting state" functional connectivity. Neuroimage 35, 396–405.

Fox, M.D., Greicius, M., 2010. Clinical applications of resting state functional connectivity. Front. Syst. Neurosci. 4, 19.

Friston, K.J., Williams, S., Howard, R., Frackowiak, R.S., Turner, R., 1996. Movement-related effects in fMRI time-series. Magn. Reson. Med. 35, 346–355.

Goetz, C.G., Tilley, B.C., Shaftman, S.R., Stebbins, G.T., Fahn, S., Martinez-Martin, P., Poewe, W., Sampaio, C., Stern, M.B., Dodel, R., Dubois, B., Holloway, R., Jankovic, J., Kulisevsky, J., Lang, A.E., Lees, A., Leurgans, S., LeWitt, P.A., Nyenhuis, D., Olanow, C.W., Rascol, O., Schrag, A., Teresi, J.A., van Hilten, J.J., LaPelle, N. & Movement Disorder Society, U.R.T.F. (2008) Movement Disorder Society-sponsored revision of the Unified Parkinson's Disease Rating Scale (MDS-UPDRS): scale presentation and clinimetric testing results. Movement Disorders, 23, 2129-2170.

Gunn, R., Coello, C., Searle, G., 2016. Molecular imaging and kinetic analysis toolbox (MIAKAT) – a quantitative software package for the analysis of PET neuroimaging data. J. Nucl. Med. 57, 1928.

Hacker, C.D., Perlmutter, J.S., Criswell, S.R., Ances, B.M., Snyder, A.Z., 2012. Resting state functional connectivity of the striatum in Parkinson's disease. Brain 135, 3699–3711.
Hall, H., Halldin, C., Guilloteau, D., Chalon, S., Emond, P., Besnard, J., Farde, L., Sedvall, G., 1999. Visualization of the dopamine transporter in the human brain postmortem with the new selective ligand [125I]PE2I. NeuroImage 9, 108–116.
Halldin, C., Erixon-Lindroth, N., Pauli, S., Chou, Y.H., Okubo, Y., Karlsson, P., Lundkvist, C., Olsson, H., Guilloteau, D., Emond, P., Farde, L., 2003. [(11)C]PE2I: a highly selective radioligand for PET examination of the dopamine transporter in monkey and human brain. Eur. J. Nucl. Med. Mol. Imaging 30, 1220–1230.
Helmich, R.C., Derikx, L.C., Bakker, M., Scheeringa, R., Bloem, B.R., Toni, I., 2010. Spatial remapping of cortico-striatal connectivity in Parkinson's disease. Cereb. Cortex 20, 1175–1186.
Herz, D.M., Eickhoff, S.B., Lokkegaard, A., Siebner, H.R., 2014. Functional neuroimaging of motor control in Parkinson's disease: A meta-analysis. Hum. Brain Mapp. 35, 3227–3237.
Hoehn, M.M., Yahr, M.D., 1967. Parkinsonism: onset, progression and mortality. Neurology 17, 427–442.
Jakobson Mo, S., Axelsson, J., Jonasson, L., Larsson, A., Ogren, M.J., Ogren, M., Varrone, A., Eriksson, L., Backstrom, D., Af Bjerken, S., Linder, J., Riklund, K., 2018. Dopamine transporter imaging with [(18)F]FE-PE2I PET and [(123)I]FP-CIT SPECT-a clinical comparison. EJNMMI Res 8, 100.
Jenkinson, M., Beckmann, C.F., Behrens, T.E., Woolrich, M.W., Smith, S.M., 2012. FSL. NeuroImage 62, 782–790.
Kish, S.J., Shannak, K., Hornykiewicz, O., 1988. Uneven pattern of dopamine loss in the striatum of patients with idiopathic Parkinson's disease. Pathophysiologic and clinical implications. N. Engl. J. Med. 318, 876–880.
Lammertsma, A.A., Hume, S.P., 1996. Simplified reference tissue model for PET receptor studies. NeuroImage 4, 153–158.
Lees, A.J., Hardy, J., Revesz, T., 2009. Parkinson's disease. Lancet 373, 2055–2066.
Li, W., Lao-Kaim, N.P., Roussakis, A.A., Martin-Bastida, A., Valle-Guzman, N., Paul, G., Loane, C., Widner, H., Politis, M., Foltynie, T., Barker, R.A., Piccini, P., 2017. C-PE2I and 18 F-Dopa PET for assessing progression rate in Parkinson's: a longitudinal study. Movement Disorders 11.
Lowe, M.J., Mock, B.J., Sorenson, J.A., 1998. Functional connectivity in single and multislice echoplanar imaging using resting-state fluctuations. Neuroimage 7, 119–132.
Luo, C., Song, W., Chen, Q., Zheng, Z., Chen, K., Cao, B., Yang, J., Li, J., Huang, X., Gong, Q., Shang, H.F., 2014. Reduced functional connectivity in early-stage drug-naive Parkinson's disease: a resting-state fMRI study. Neurobiol. Aging 35, 431–441.
Manza, P., Zhang, S., Li, C.S., Leung, H.C., 2016. Resting-state functional connectivity of the striatum in early-stage Parkinson's disease: Cognitive decline and motor symptomatology. Hum. Brain Mapp. 37, 648–662.
Marek, K., Innis, R., van Dyck, C., Fussell, B., Early, M., Eberly, S., Oakes, D., Seibyl, J., 2001. [123I]beta-CIT SPECT imaging assessment of the rate of Parkinson's disease progression. Neurology 57, 2089–2094.
Mazziotta, J.C., Toga, A.W., Evans, A., Fox, P., Lancaster, J., 1995. A probabilistic atlas of the human brain: theory and rationale for its development. The International Consortium for Brain Mapping (ICBM). NeuroImage 2, 89–101.
Nurmi, E., Ruottinen, H.M., Bergman, J., Haaparanta, M., Solin, O., Sonninen, P., Rinne, J.O., 2001. Rate of progression in Parkinson's disease: A 6-[18F]fluoro-L-dopa PET study. Movement Disorders 16, 608–615.
Nurmi, E., Ruottinen, H.M., Kaasinen, V., Bergman, J., Haaparanta, M., Solin, O., Rinne, J.O., 2000. Progression in Parkinson's disease: a positron emission tomography study with a dopamine transporter ligand [18F]CFT. Ann. Neurol. 47, 804–808.
Olde Dubbelink, K.T., Schoonheim, M.M., Deijen, J.B., Twisk, J.W., Barkhof, F., Berendse, H.W., 2014. Functional connectivity and cognitive decline over 3 years in Parkinson disease. Neurology 83, 2046–2053.
Parkinson Study, G., 2002. Dopamine transporter brain imaging to assess the effects of pramipexole vs levodopa on Parkinson disease progression. JAMA 287, 1653–1661.
Pavese, N., Brooks, D.J., 2009. Imaging neurodegeneration in Parkinson's disease. BBA 1792, 722–729.
Piccini, P.P., 2003. Dopamine transporter: basic aspects and neuroimaging. Movement Disorders 18 (Suppl. 7), S3–8.
Politis, M., 2014. Neuroimaging in Parkinson disease: from research setting to clinical practice. Nat. Rev. Neurol. 10, 708–722.
Power, J.D., Barnes, K.A., Snyder, A.Z., Schlaggar, B.L., Petersen, S.E., 2012. Spurious but systematic correlations in functional connectivity MRI networks arise from subject motion. Neuroimage 59, 2142–2154.
Rieckmann, A., Gomperts, S.N., Johnson, K.A., Growdon, J.H., Van Dijk, K.R., 2015. Putamen-midbrain functional connectivity is related to striatal dopamine transporter availability in patients with Lewy body diseases. Neuroimage Clin. 8, 554–559.
Rolinski, M., Griffanti, L., Szewczyk-Krolikowski, K., Menke, R.A.L., Wilcock, G.K., Filippini, N., Zamboni, G., Hu, M.T.M., Mackay, C.E., 2015. Aberrant functional connectivity within the basal ganglia of patients with Parkinson's disease. Neuroimage-Clin. 8, 126–132.
Ruan, W.W., Sun, X., Liu, F., Zhang, Y.X., Lan, X.L., 2019. Regional comparison to differentiate Parkinson's disease and multiple system atrophy by hybrid PET/MR. J. Nucl. Med. 60.
Seibyl, J.P., Marek, K.L., Quinlan, D., Sheff, K., Zoghbi, S., Zea-Ponce, Y., Baldwin, R.M., Fussell, B., Smith, E.O., Charney, D.S., van Dyck, C., et al., 1995. Decreased single-photon emission computed tomographic [123I]beta-CIT striatal uptake correlates with symptom severity in Parkinson's disease. Ann. Neurol. 38, 589–598.
Shih, M.C., Hoexter, M.Q., Andrade, L.A., Bressan, R.A., 2006. Parkinson's disease and dopamine transporter neuroimaging: a critical review. Sao Paulo Med. J. 124, 168–175.
Shine, J.M., Bell, P.T., Matar, E., Poldrack, R.A., Lewis, S.J.G., Halliday, G.M., O'Callaghan, C., 2019. Dopamine depletion alters macroscopic network dynamics in Parkinson's disease. Brain 142, 1024–1034.
Surmeier, D.J., Shen, W., Day, M., Gertler, T., Chan, S., Tian, X., Plotkin, J.L., 2010. The role of dopamine in modulating the structure and function of striatal circuits. Prog. Brain Res. 183, 149–167.
Szewczyk-Krolikowski, K., Menke, R.A., Rolinski, M., Duff, E., Salimi-Khorshidi, G., Filippini, N., Zamboni, G., Hu, M.T., Mackay, C.E., 2014. Functional connectivity in the basal ganglia network differentiates PD patients from controls. Neurology 83, 208–214.
Tondo, G., Esposito, M., Dervenoulas, G., Wilson, H., Politis, M., Pagano, G., 2019. Hybrid PET-MRI Applications in Movement Disorders. Int. Rev. Neurobiol. 144, 211–257.
Tziortzi, A.C., Searle, G.E., Tzimopoulou, S., Salinas, C., Beaver, J.D., Jenkinson, M., Laruelle, M., Rabiner, E.A., Gunn, R.N., 2011. Imaging dopamine receptors in humans with [11C]-(+)-PHNO: dissection of D3 signal and anatomy. Neuroimage 54, 264–277.
Wu, T., Wang, J., Wang, C., Hallett, M., Zang, Y., Wu, X., Chan, P., 2012. Basal ganglia circuits changes in Parkinson's disease patients. Neurosci. Lett. 524, 55–59.
Wu, T., Wang, L., Chen, Y., Zhao, C., Li, K., Chan, P., 2009. Changes of functional connectivity of the motor network in the resting state in Parkinson's disease. Neurosci. Lett. 460, 6–10.